

ENERGY EFFICIENT CASCADE PREDICTIVE VEHICLE STABILITY CONTROL

Justin Sill and Beshah Ayalew

Clemson University-International Center for Automotive Research
 Greenville, SC 29607

jsill@clemson.edu, beshah@clemson.edu

ABSTRACT

This paper presents a predictive vehicle directional stability control structure that has integrated energy-loss reduction benefits during transient handling maneuvers. The method is based on the idea of balancing longitudinal and lateral tire force saturation levels using a cascade model predictive structure for the optimal distribution of tractive or braking torques. Balancing saturation levels also has the added benefit of reducing and evening-out tire wear. To demonstrate the energy-loss reduction benefits, we consider nonlinear simulations of a nominally unstable truck featuring an independent drive system. Comparisons against a commonly cited brake-based yaw stability control strategy with similar directional control performance shows that the proposed predictive saturation management approach provides energy-loss reductions of more than 60%. This energy efficiency benefits are retained whether or not the drive system has regenerative/energy recovery capabilities.

Keywords: cascade MPC, vehicle stability control, tire saturation, independent drive

NOMENCLATURE

A, B, C, E Linearized model matrices
 A Cross-sectional area
 A_{eq}, B_{eq} Equality constraint matrices
 b_i Viscous wheel damping
 C_D Aerodynamic drag coefficient
 C_α Lateral cornering stiffness
 C_x Longitudinal slip stiffness
 d_f Front track width
 d_r Rear track width
 $\Delta E_{kinetic}$ Change in kinetic energy
 E_{loss} Energy loss due to tires
 FMVSS: Federal Motor Vehicle Safety Standards
 F_x Longitudinal tire force
 $F_{y,f}$ Front axle lateral force
 $F_{y,r}$ Rear axle lateral force
 I_w Tire/wheel rotational inertia
 J Cost/objective function

J_z Vehicle yaw inertia
 K_1, K_2 Tire property coefficients
 l_f Distance from CG to front axle
 l_r Distance from CG to rear axle
 m Vehicle mass
 M_y Corrective yaw moment
 Q_l Instant weighting matrix for low-level MPC
 Q Expanded weighting matrix for low-level MPC
 $Q_{\alpha,l}$ Instant weighting matrix for high-level MPC
 Q_α Expanded weighting matrix for high-level MPC
 R_w Tire Radius
 T_i Individual wheel torque
 u Control input
 Δu Control input increment
 U Expanded control input for prediction
 ΔU Expanded control input increment for control horizon
 VSC Vehicle Stability Control
 V_x Longitudinal vehicle velocity
 V_y Lateral vehicle velocity
 $W_{t,i}$ Individual work of applied wheel torque
 W_{aero} Work of aerodynamic drag force
 W_{RR} Work of rolling resistance
 x Predicted state vector
 y Predicted output vector
 Y Predicted output vector for entire prediction horizon
 α Lateral slip angle
 α_{sat} Lateral tire saturation
 γ, ζ, Ω Prediction matrices
 δ Road wheel steering
 ψ yaw angle
 κ Longitudinal tire saturation
 σ Longitudinal slip ratio
 ρ Air density
 ω_i Individual wheel spin

INTRODUCTION

The safety benefits of vehicle directional stability control systems are now well recognized as is evident with the adoption of the FMVSS 126 rule requiring electronic stability control

systems for all new light vehicles sold in the US[1]. The most common implementations of these stability control systems involve brake-based solutions where the necessary corrective yaw moments are generated using differential braking. Proposed alternative implementations include active front and rear steering [2-4], active and semi-active suspensions [5, 6] and variations of active torque management [7-9]. In most of these works, consideration of the force generation capability is limited, at most, to friction estimation and subsequent adjustment of reference targets and control gains.

In this paper, we consider a direct and predictive consideration of tire force-capability in the design of the vehicle stability control (VSC) structure. Our approach is particularly suited for advanced and emerging vehicles with powertrains incorporating independently controlled wheel/axle drives (e.g. in-wheel or hub motors[10]). These power trains offer increased energy-efficiency, reliability and packaging benefits. The specific purpose of this paper, however, is to demonstrate that the proposed predictive stability control structure in itself provides additional energy-loss reduction benefits by balancing and reducing the tire-force saturation levels among all tires of the vehicle.

Our approach involves defining longitudinal and lateral tire force saturation levels as quantities that can be estimated using tire force and slip angle estimation schemes that have already been proposed and demonstrated in the literature [11-15]. These schemes rely on readily available vehicle dynamics sensors (yaw rate, lateral acceleration, wheel speeds) and reduced-order vehicle and tire/wheel dynamics models. Given the saturation levels, we then set up a two-level model predictive control (MPC) structure with cascaded optimization objectives of balancing these saturation levels among all the tires of the vehicle in determining the optimal drive torque distribution. For the first, high-level MPC, we set the objective as that of re-balancing the per-axle lateral force saturations. This objective is motivated by the observation that such front/rear lateral force saturation differentials are directly related to the understeer/ oversteer behavior of the vehicle, as we showed in our previous work[16]. The second, low-level MPC is given the objective of balancing the longitudinal tire force saturation levels so that no one tire is unnecessarily oversaturated. This latter objective is constrained by the high-level stabilization objective as well as the driver demanded torque for maintaining forward speed.

It turns out that this idea of balancing tire force saturation levels has an inherent energy-loss reduction benefit. This is because the optimal distribution of drive torque that minimizes saturation imbalances reduces unnecessary overtaxing of any one tire that has already saturated. Such a tire cannot generate any more force but will simply operate in the dissipative sliding zone. The proposed approach re-distributes the demand to the still capable tire(s) with less saturation levels. This allocation of the drive torques is best done in a predictive framework where assumptions are made about the tire-behavior vis-a-vis tire-behavior prediction models. In this work, we assume that such

models (e.g. Pacejka models[17]) are available, at a minimum, as look up tables of the relevant cornering and slip stiffness's vs. slip quantities as we detail below.

The rest of the paper is organized as follows. First, we formally define tire-force saturation for our purposes and discuss the proposed cascade MPC strategy that uses these saturation levels in the optimization objectives. We then apply the strategy to a nonlinear 7 DOF handling model of a medium duty truck featuring independent wheel drive. For the purposes of comparison, we also consider a conventional brake-based stability control strategy. Comparative results are presented and discussed, and finally, we provide the conclusions of the work.

DEFINITION OF TIRE FORCE SATURATION

The saturation level characterizes the deficiency of a tire to generate a force that increases linearly with slip (see Fig. 1).

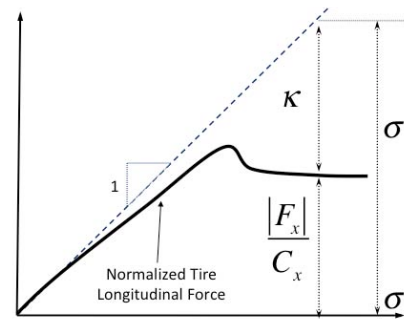


FIGURE 1 DEFINITION OF LONGITUDINAL TIRE SATURATION

The longitudinal tire force saturation is defined by:

$$\kappa_i = \sigma_i - \frac{F_{x,i}}{C_{x,i}} \quad (1)$$

where, σ_i is the tire/wheel longitudinal slip ratio; $F_{x,i}$ is the longitudinal tire force; and $C_{x,i}$ is the slip stiffness of the tire. Saturation of the lateral force can be defined similarly. For the purposes of this paper, only the per-axle lateral force saturations are relevant and are defined by:

$$\alpha_{sat} = \alpha - \frac{F_y}{C_\alpha} \quad (2)$$

where, α is the (front or rear) axle slip angle, F_y is the axle lateral force and C_α is the axle cornering stiffness. We again note that both the forces and slip quantities are assumed known via one or more of the various estimation methods cited earlier. We also note that at high slip values corresponding to predominantly (dissipative) sliding zones on the tire-road contact patches, the saturation levels grow drastically.

CASCADE MPC FOR VSC

Model predictive control (MPC) is receiving increasing attention in vehicle dynamics control, particularly for autonomous vehicle applications[18-22]. MPC uses the system's model to predict the system's response to suitably parameterized future control inputs, and makes optimization decisions that lead to the selection of the optimal control inputs that achieve some desired objective without violating constraints[23]. In this work, we propose and implement a two-level cascade MPC structure for vehicle stability control. The scheme is shown in Fig. 2.

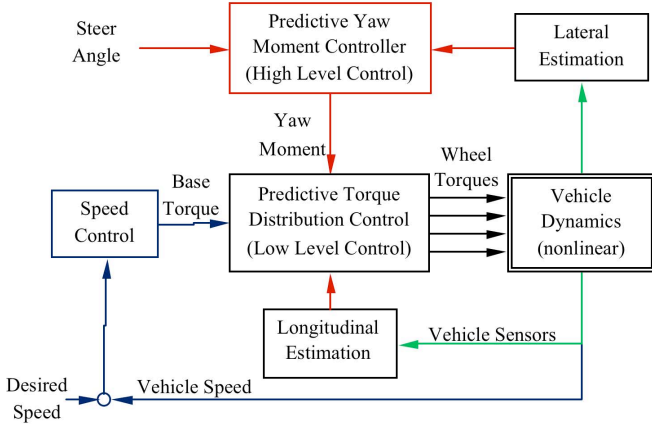


FIGURE 2 CASCADE MPC FOR VSC

This cascade MPC structure is motivated by physical grounds and exploits the natural time-scale separation of the rotational dynamics of the tire/wheel system (faster) from that of the lateral dynamics of the vehicle (slower). As already mentioned, the high-level control determines the necessary corrective yaw moment in away that balances the lateral force saturations between the front and rear axles. This serves to correct oversteer/understeer. The low-level control determines the drive/brake torque distributions that balance the individual longitudinal tire force saturations. The distribution is constrained by the (driver demanded) speed control torque as well as the corrective yaw moment needs determined by the high-level MPC. Each level of the cascade follows established MPC computational steps we briefly describe below. The reader is referred to the text book [23] for detailed discussions of MPC.

Low-level MPC

The presence of distinct longitudinal saturations is unavoidable when using driving/braking distributions to achieve yaw corrections while meeting forward speed demands. Instead, in determining the optimal torque distributions, we can set the objective to be that of balancing the saturation levels among all tires. A suitable cost function for this objective is computed as the cumulative deviation of the individual longitudinal saturations from their average:

$$J = \left[\sum_{i=LF,RF,LR,RR} \left(\kappa_i - \frac{\sum_{j=LF,RF,LR,RR} \kappa_j}{4} \right)^2 \right] \quad (3)$$

This can be re-written in the usual quadratic matrix form as:

$$J = \bar{\kappa}^T Q_1 \bar{\kappa}, \quad Q_1 = \begin{bmatrix} 0.75 & -0.25 & -0.25 & -0.25 \\ -0.25 & 0.75 & -0.25 & -0.25 \\ -0.25 & -0.25 & 0.75 & -0.25 \\ -0.25 & -0.25 & -0.25 & 0.75 \end{bmatrix} \quad (4)$$

where, $\bar{\kappa}$ is a vector of the individual longitudinal tire saturations, and Q_1 is the constant positive semi-definite matrix as given. It is possible to include additional terms that penalize the magnitudes of the individual saturation levels, which will give a different positive (semi-definite) definite matrix Q_1 . However, we found the above form sufficient for our purposes here.

The two constrains of the low-level torque distribution MPC are:

$$\left[\begin{array}{cccc} \frac{d_f}{2R_w} & \frac{d_f}{2R_w} & -\frac{d_r}{2R_w} & -\frac{d_r}{2R_w} \end{array} \right] \left\{ \begin{array}{c} F_{x,LF} \\ F_{x,RF} \\ F_{x,LR} \\ F_{x,RR} \end{array} \right\} = M_\psi \quad (5)$$

$$\sum_{i=LF,RF,LR,RR} T_i = T_{total} \quad (6)$$

where, d_f and d_r are the track widths; R_w is the effective tire radius; $F_{x,i}$ is the individual wheel forces; M_ψ is the corrective yaw moment determined by the high-level control; T_i is the individual wheel torques; and T_{total} is the total commanded base torque (for driver/forward speed control). Additional softer constraints on the increment of the wheel torques can be added to limit the rate of change of the wheel torque to values achievable by the physical actuators/motors. The low-level MPC optimization problem can be cast in standard form as follows:

$$\begin{aligned} & \min_{\Delta U} (Y^T Q Y + (\Delta U)^T R (\Delta U)) \\ & \text{subjected to:} \\ & x_{k+1} = f(x_k, u_k, \Delta u_k) \\ & \bar{\kappa}_{k+1} = g(x_{k+1}, u_k, \Delta u_k) \\ & A_{eq} \Delta U = B_{eq} \end{aligned} \quad (7)$$

$$Y = \left\{ \begin{array}{c} \bar{\kappa}_{k+1} \\ \vdots \\ \bar{\kappa}_{k+H_p} \end{array} \right\}; \quad \Delta U = \left\{ \begin{array}{c} u_{k+1} - u_k \\ \vdots \\ u_{k+H_u} - u_k \end{array} \right\}^T = \left\{ \begin{array}{c} \Delta u_k \\ \vdots \\ \Delta u_{k+H_p} \end{array} \right\}^T$$

where, the functions f and g define the predictive vehicle and tire/wheel dynamics model (whose linearization is described below); u is a vector of the four wheel torques with control horizon H_u ; x is a vector of the system states that include the

forward velocity, four wheel spins, and four longitudinal tire forces; Y is a system output vector which is a concatenation of the individual tire saturations into the future prediction horizon H_p ; A_{eq} and B_{eq} are constant matrices that define the equality constraints; Q and R are weighting matrices to be defined below. In this work, we set the control horizon to be equal to the prediction horizon.

The selection of the prediction horizon H_p should consider the specifics of the physical process. In the present case, the main considerations include a priori unknown future exogenous inputs, such as the driver inputs of steering and commanded base torque, and the uncertainty associated with the linearization of the vehicle and tire models. A remedy adopted here is to consider a short prediction horizon (of 0.1 seconds) implemented in a receding horizon scheme with fast update cycles (of 0.01 seconds) so the most recent information of these inputs can be used and the effects of the linearization and driver command sampling errors can be minimized.

The linearization of the longitudinal vehicle dynamics gives:

$$\dot{V}_x = \frac{\sum_{i=LF,RF,LR,RR} F_{x,i} - \rho C_D A V_{x,0} V_x + \frac{1}{2} \rho C_D A V_{x,0}^2}{m} \quad (8)$$

where V_x is the vehicle's forward velocity, $F_{x,i}$ are the longitudinal tire forces; ρ is air density; C_D and A is the vehicle's drag coefficient and cross-sectional area; $V_{x,0}$ is the vehicle's velocity at the point of linearization (current state). For the tire/wheel rotational dynamics of each of the four tires:

$$\dot{\omega}_i = \frac{T_i - F_{x,i} R_w - b_i \omega_i}{I_w} \quad \text{for } i = LF, RF, LR, RR \quad (9)$$

where, the T_i is the controlled torque, R_w is the effective tire radius, and b_i is wheel viscous damping.

The longitudinal tire force saturation defined earlier includes the longitudinal tire forces. It is desirable to formulate state equations for these forces. The longitudinal force dynamics can be constructed considering that these forces are functions of both the vehicle speed and tire/wheel spin. Then:

$$\dot{F}_{x,i} = \frac{\partial F_{x,i}}{\partial \sigma_i} \frac{\partial \sigma_i}{\partial \omega_i} \dot{\omega}_i + \frac{\partial F_{x,i}}{\partial \sigma_i} \frac{\partial \sigma_i}{\partial V_x} \dot{V}_x = K_{1,i} \dot{\omega}_i + K_{2,i} \dot{V}_x \quad (10)$$

where, the coefficients K_1 and K_2 are determined from a nonlinear representation of the tire force/slip curve and partial derivatives of the slip ratio at the linearization point (given by $V_{x,0}$ and $\omega_{i,0}$). The gradient of the tire force with respect to slip ratio is a form of effective slip stiffness that can be implemented using a simple lookup table based on the current estimate of slip ratio at the linearization point. The look up table is to be obtained from tire test data or its analytical representations (e.g. Pacejka models).

The defining equations of the longitudinal saturations are linearized at the current states as follows:

$$\kappa_i = -\frac{\omega_{i,0} R_w}{V_{x,0}^2} V_x + \frac{R_w}{V_{x,0}} \omega_i - \frac{1}{C_{x,i}} F_{x,i} + \frac{\omega_{i,0} R_w - V_{x,0}}{V_{x,0}} \quad (11)$$

Equations (8)-(11) can be written in linear state space form and subsequently discretized for use as the predictive model for MPC. Details of these steps are given in [24]. To proceed, we write the resulting model in the form:

$$x_{k+1} = Ax_k + B_1 u_k + B_2 \quad (12)$$

$$y_{k+1} = Cx_k + E_1 \quad (13)$$

where, the matrices of A , B_1 , B_2 , C , and E_1 are updated based on the linearization of the system at each control update cycle. Here, y is the output vector of the longitudinal saturations. By expanding the state and output vectors into the prediction horizon, the predicted outputs can be assembled in the compact form:

$$Y = \gamma x_k + \Omega u_{k-1} + \zeta \Delta U + \bar{E} \quad (14)$$

where Y and ΔU are concatenations of the predicted saturation outputs and wheel torque (control input) increments, respectively, through the prediction horizon; matrices γ , Ω , ζ , and \bar{E} are constant during one control update/iteration; x_k and u_{k-1} are the current states and previous control inputs, respectively.

Substituting (14) in the optimization problem (7), expanding, simplifying, collecting terms, and neglecting constant additive terms, the optimization problem reduces to a quadratic form:

$$\min_{\Delta U} \left\{ \begin{array}{l} (\Delta U)^T [\zeta^T Q \zeta + R] (\Delta U) \\ + [(\zeta x_k)^T Q \zeta + (\Omega u_k)^T Q \zeta + \bar{E}^T Q \zeta \\ + (x_k \gamma Q)^T \zeta + (u_k \Omega Q)^T \zeta + (\bar{E} Q)^T \zeta] \Delta U \end{array} \right\} \quad (15)$$

subjected to:

$$A_{eq} \Delta U = B_{eq}$$

where, the weighing matrix Q considers the saturation management objective (as concatenations of Q_i given by Eq(4) into the prediction horizon); and R is a diagonal of control weights which affect the soft constraint on the rate of change of the input torques. The equality constraints of total torque and corrective yaw moment given previously ((5) and (6)) can be expressed in terms of the control input increment for the prediction horizon. The steps for doing this (i.e., for extracting A_{eq} and B_{eq} in (15)) are detailed in [24]. The optimization problem in (15) can be easily solved for the wheel torque increments, ΔU , using quadratic optimization software tools. The MPC scheme updates this solution (including the linearizations) at each control update cycle. For the torque distribution problem, this update is done at 100 Hz (or every 0.01sec).

High-level MPC

We incorporate the definition of axle lateral force saturation given earlier into an appropriate objective function for the high-level vehicle stability control. Proceeding as before, the objective is set as one of minimizing the deviation of the lateral axle saturation levels from their average. The cost function is given by:

$$J = \left[\sum_{i=F,R} \left(\alpha_{sat,i} - \frac{\sum_{j=F,R} \alpha_{sat,j}}{2} \right)^2 \right] \quad (16)$$

This can then be rewritten in quadratic matrix form as:

$$J = \bar{\alpha}_{sat}^T Q_{\alpha,1} \bar{\alpha}_{sat} \quad Q_{\alpha,1} = \begin{bmatrix} 0.5 & -0.5 \\ -0.5 & 0.5 \end{bmatrix} \quad (17)$$

where, $Q_{\alpha,1}$ is a constant positive semi-definite matrix and $\bar{\alpha}$ is a vector of the lateral axle saturations. The optimization problem for the MPC is then posed as:

$$\min_U \{ Y^T Q Y + U^T R U \}$$

subjected to:

$$x_{k+1} = f(x_k, u_k) \quad (18)$$

$$y_{k+1} = g(x_k, u_k)$$

$$U_{LB} < U < U_{UB}$$

$$U = \begin{bmatrix} u_k \\ \vdots \\ u_{k+H_u} \end{bmatrix}^T = \begin{bmatrix} M_{\psi,k} \\ \vdots \\ M_{\psi,k+H_u} \end{bmatrix}^T; \quad Y = \begin{bmatrix} \bar{\alpha}_{sat,k+1} \\ \vdots \\ \bar{\alpha}_{sat,k+1+H_p} \end{bmatrix}$$

where, the functions f and g represent the lateral handling model of the vehicle used as the prediction model; U is the vector of corrective yaw moments over the control horizon H_u ; Y is the lateral axle saturations expanded into the prediction horizon H_p ; and U_{LB} and U_{UB} are the upper and lower bounds of the control input and limit the corrective yaw moment to physically achievable values.

There are two structural differences of this objective function compared to that of the torque distribution control problem of the previous section. First, the penalty weight, R , on the control input is applied to the absolute magnitude of the control input but not to the increment of control. In our simulations, formulations including increment terms did not significantly improve performance. Furthermore, there is a fundamentally different goal in formulating the penalty in this manner. In the torque distribution control, it was desired to not significantly change the torque unless it was necessary, while in the present yaw moment control we penalize any magnitude of the corrective yaw moment (not just its increment). Secondly, there are no equality constraints for the present optimization to satisfy, but limiting bounds are selected considering the capability of the vehicle to be controlled.

The predictive model we use for lateral handling dynamics is a single-track vehicle model at constant forward velocity:

$$\begin{aligned} \dot{V}_y &= \frac{(F_{yF} + F_{yR})}{m} - V_{x,0} \dot{\psi} \\ \ddot{\psi} &= \frac{(F_{yF} l_f - F_{yR} l_r) + M_{\psi}}{J_z} \end{aligned} \quad (19)$$

where, V_y and $\dot{\psi}$ are the states of lateral velocity and yaw rate; the F_{yF} and F_{yR} are the front and rear axle lateral forces; m is the total vehicle mass; $V_{x,0}$ is the current estimate of the forward velocity; J_z is the yaw inertia; l_f and l_r are the distances from the vehicle's c.g. to the front and rear axle, respectively; M_{ψ} is a corrective yaw moment to be determined by the predictive control.

The lateral force is a nonlinear function of lateral velocity and yaw rate, which together define the axle slip angles. A simple first-order relaxation length model [25] was used to address the delay between the generation of lateral slip angle and the corresponding force. Linearization of this force dynamics leads to:

$$\begin{aligned} \dot{F}_{y,F} &= \frac{V_{x,0}}{\lambda_F} \left[\frac{\partial f_{y,F}}{\partial \alpha} \Big|_{\alpha_{F,0}} \left(\frac{\partial \alpha_F}{\partial V_y} \Big|_{V_{y,0}} + \frac{\partial \alpha_F}{\partial \dot{\psi}} \Big|_{\dot{\psi}_0} - \delta \right) - F_{y,F} \right] \\ \dot{F}_{y,R} &= \frac{V_{x,0}}{\lambda_R} \left[\frac{\partial f_{y,R}}{\partial \alpha} \Big|_{\alpha_{R,0}} \left(\frac{\partial \alpha_R}{\partial V_y} \Big|_{V_{y,0}} + \frac{\partial \alpha_R}{\partial \dot{\psi}} \Big|_{\dot{\psi}_0} \right) - F_{y,R} \right] \end{aligned} \quad (20)$$

where, λ_F and λ_R are the front and rear relaxation lengths, respectively; $f_{y,F}$ and $f_{y,R}$ are the nonlinear functions describing tire lateral force versus slip angle; α_F and α_R are the front and rear axle slip angles, respectively; and δ is the road wheel steering angle (front steered vehicle). Substituting the definitions for the axle slip angles [26], the lateral axle force dynamics can be expressed in-terms of the yaw rate and lateral velocity:

$$\begin{aligned} \dot{F}_{y,F} &= \frac{V_{x,0}}{\lambda_F} \left(-C_1 \left(\frac{V_y + l_f \dot{\psi}}{V_{x,0}} - \delta \right) - F_{y,F} \right) \\ \dot{F}_{y,R} &= \frac{V_{x,0}}{\lambda_R} \left(-C_2 \left(\frac{V_y - l_r \dot{\psi}}{V_{x,0}} \right) - F_{y,R} \right) \end{aligned} \quad (21)$$

where, C_1 and C_2 are the partial derivatives of the tire force functions versus slip angle and represent the effective axle cornering stiffnesses at the operating points (current states). Again, these can be implemented through look up tables, and constitute a major simplification in the predictive model. The values of these stiffnesses are to be updated at each iteration/update of the controller.

For the implementation of the lateral axle saturations in the objective function, it is desirable to have the axle saturations as

outputs. From the definitions of axle saturation given by Eq (2), the linearized front and rear axle saturations are given as outputs of the state-space handling model (19&21) as follows:

$$\begin{Bmatrix} \alpha_{sat,F} \\ \alpha_{sat,R} \end{Bmatrix} = \begin{bmatrix} \frac{1}{V_{x,0}} & \frac{l_f}{V_{x,0}} & -\frac{1}{C_1} & 0 \\ \frac{1}{V_{x,0}} & -\frac{l_r}{V_{x,0}} & 0 & -\frac{1}{C_2} \end{bmatrix} \begin{Bmatrix} V_y \\ \dot{\psi} \\ F_{yf} \\ F_{yr} \end{Bmatrix} + \begin{bmatrix} -\delta \\ 0 \end{bmatrix} \quad (22)$$

Using this linearized state space model, discretizing, and proceeding in similar steps as above, the forward prediction can be written compactly as:

$$Y = \gamma x_k + \zeta U + \bar{E} \quad (23)$$

where, Y is a concatenation of axle saturation levels through the prediction horizon; U is a vector of the corrective yaw moments for the horizon; the matrices of γ , ζ , and \bar{E} have similar interpretations as before. With this, the optimization problem for the high-level MPC can be re-written as:

$$\min_U \left\{ \begin{aligned} &U^T [\zeta^T Q \zeta + R] U + [(\zeta x_k)^T Q \zeta + \bar{E}^T Q \zeta] \\ &+ (x_k \gamma Q)^T \zeta + (\bar{E} Q)^T \zeta U \end{aligned} \right\} \quad (24)$$

subject to:

$$U_{LB} < U < U_{UB}$$

This formulation is different from standard MPC formulations[23] due to the constants (\bar{E}) in the prediction model. The optimal control input U that minimizes the objective can be readily obtained through quadratic programming methods.

The prediction horizon for the high-level MPC is chosen as 0.5 sec and its control update interval is chosen to be 0.1 sec and this is consistent with the short prediction horizon of the low-level control. For the optimizations conducted at each update, we assume that the remaining exogenous input (the steering input in the case of the high-level control) remains constant during the prediction horizon. Simulations suggest that the fast control updates (every 0.1 sec) help compensate for limitations of this assumption.

RESULTS AND DISCUSSIONS

Vehicle and Maneuver

For the purpose of demonstrating the performance of the proposed cascade MPC saturation management strategy, we applied the strategy to a simulation model of a medium duty truck with a GVW of 8000 lbs and with a powertrain featuring independent wheel drives (4x4). This vehicle has a high center of gravity and easily approaches oversteer conditions during transient maneuvers on dry asphalt road. The mathematical vehicle model exercised in these analysis is a 7 DOF (body yaw, lateral and longitudinal motions, and 4 tire/wheel rotations)

nonlinear model and is described elsewhere[20]. We also adopt an open-loop “sine with dwell” maneuver that has been defined by NHTSA [1] to emulate a severe obstacle avoidance type maneuver for the purpose of evaluating VSC systems. This input induces a dynamic nonlinear response featuring high sideslip for the uncontrolled vehicle.

Comparison VSC strategy

By way of comparison, we consider a traditional PI-type yaw rate reference controller [2, 12] to substitute the high-level yaw rate reference controller of the cascade MPC structure. In addition, the low-level controller is substituted with a rule-based controller that achieves the desired corrective yaw moment by differential braking of the individual tires. This cascade of yaw rate reference (high-level) and rule-based brake (low-level) control strategy is tuned to give similar stabilizing performance as the cascade MPC discussed in this paper. This is shown in Fig 3. The same driver (speed controller) was used for the both cases.

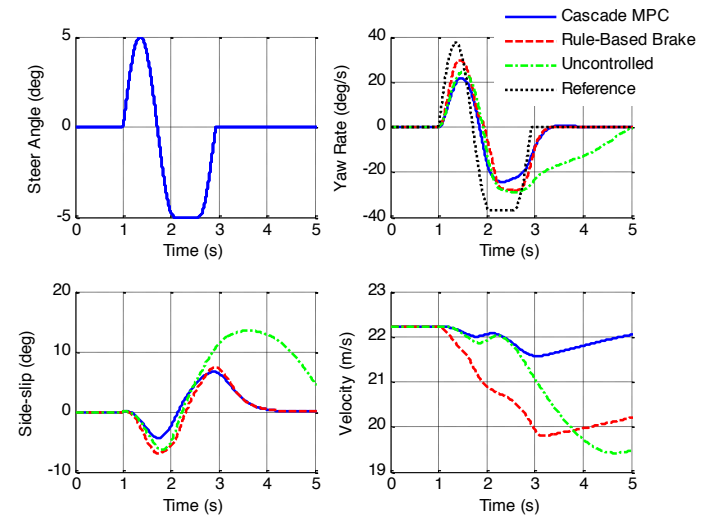


FIGURE 3. COMPARISON OF PERFORMANCE

In this comparison (Fig.3), it should be noted that the two controllers both stabilize the vehicle but work differently. The goal of the rule-based control is to force the vehicle to obtain the desired reference yaw rate and does not take into consideration the handling balance or tire/axle force capability. It consequently sacrifices efficiency as demonstrated by higher vehicle side-slip angles and larger reductions in forward velocity. Conversely, the cascade MPC strategy does not use a reference yaw rate. Instead, it stabilizes the vehicle by achieving a balance of saturations and therefore involves a more efficient use of the available tire traction as indicated by the lower side-slip angles and lower reduction in forward velocity.

Control Efforts and Energy Losses

Figure 4 shows the corrective yaw moments and individual torques applied by the two stability control structures during the maneuver. It can be seen that the cascade MPC strategy proposed

here involves lower control magnitudes than the rule-based brake approach, in terms of both the high-level corrective yaw moment and the low-level individual wheel torques.

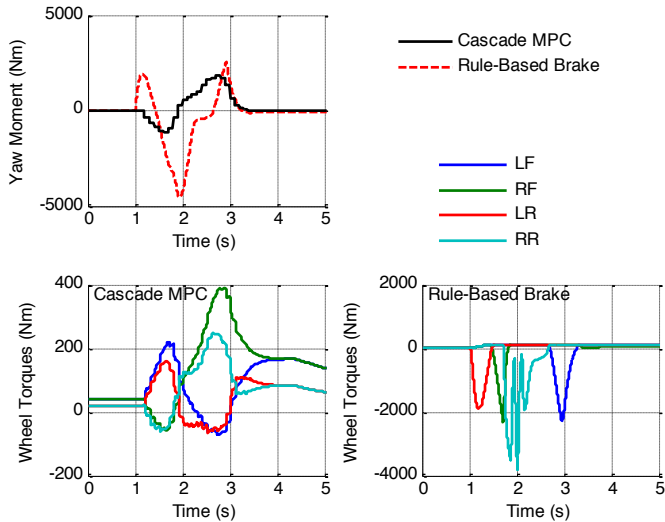


FIGURE 4. CORRECTIVE YAW MOMENT AND INDIVIDUAL WHEEL TORQUES UNDER THE TWO STRATEGIES

We also computed the energy losses for the vehicle when undergoing the same maneuver under the two stability control structures. The energy losses are computed by:

$$E_{loss} = \sum_{i=LF,RF,LR,RR} W_{T,i} - W_{Aero} - W_{RR} - \Delta E_{kinetic} \quad (25)$$

Here, the first term is the total work done by the individual wheel torques, the second and third terms are aerodynamic and rolling resistance losses, respectively, and the last term is the net change in the total kinetic energy of the vehicle system during the maneuver. The net loss is the dissipation at the tire-ground contact patches (non-conservative work done by the tire forces).

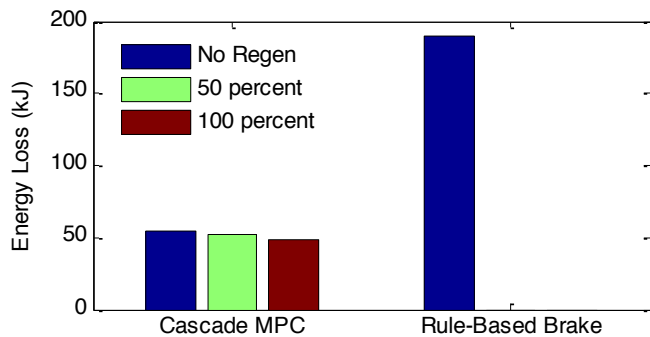


FIGURE 5. ENERGY LOSSES UNDER THE TWO STRATEGIES

Figure 5 shows the energy losses under the two VSC structures. We also included cases where all (no regen) or half

(50% regen) of the regenerative braking torques of the cascade MPC structure are assumed lost due to some inefficiency of the drive system. It can be seen that the cascade MPC structure involves significantly lower energy losses than the traditional structure and this advantage remains even if the independent drive system has significant inefficiencies (even if it is completely dissipative with no regen). This implies that lower energy loss benefits come from the more efficient use of tire traction capability by the cascade MPC structure.

This last point is also confirmed by comparing the longitudinal tire saturation levels shown in Fig 6. The cascade MPC maintains low-levels of tire saturations, across all tires, as it is designed to do. The rule-based brake strategy, on the other hand, involves excessive saturations on individual tires for the aggressive differential braking needed to generate the high corrective yaw moments necessary to stabilize the vehicle.

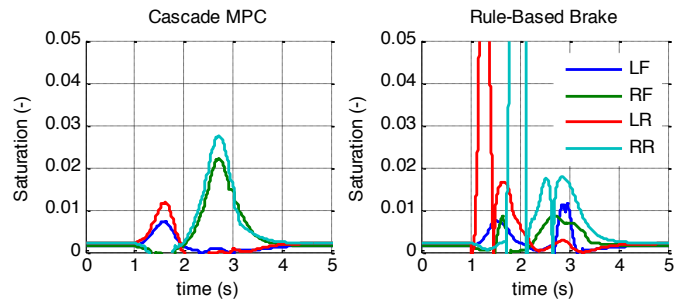


FIGURE 6. LONGITUDINAL SATURATIONS UNDER THE TWO STRATEGIES

CONCLUSIONS

In this paper, we proposed a cascade MPC strategy for vehicle stability control that embeds energy-loss reducing features. The strategy is envisaged for vehicles featuring independent wheel drives where it is possible to distribute drive/brake torques in such away as to balance tire-force saturation levels. Our approach assigned the objective of balancing lateral force saturation levels to a high-level controller that determines the necessary corrective yaw moment, which is then passed as a constraint to a low-level controller whose objective is balancing longitudinal tire force saturations.

The results show that for a standard transient handling maneuver, the presented cascade MPC strategy involves less energy losses through the maneuver than a traditional yaw-rate error correcting, brake-based VSC strategy. This is explained further by looking at individual tire saturation levels, which remained low with the cascade MPC strategy (due to reduced operation in sliding dominated regimes). The results also indicate that the absence or in efficiency of regenerative capability have relatively low impact on the energy-loss reduction benefits.

A number of aspects of this proposed approach require further exploration including, but not limited to: load adaptability

for tire-model parameters, constrained optimizations that embed regenerative limitations, real-time solvability of the cascade MPC on control prototyping and commercial hardware (ECUs).

REFERENCES

- [1] NHTSA, 2007. "Federal Motor Vehicle Safety Standards: Electronic Stability Control Systems, Final Rule", FMVSS 126, NHTSA 49 CFR Parts 571 and 585.
- [2] Ghoneim, Y., Lin, W., Sidlosky, D., Chen, H., Chin, Y.-K. and Tedrake, M., 2000. "Integrated Chassis Control System to Enhance Vehicle Stability". *International Journal of Vehicle Design*. 23(1/2): pp. 124-144.
- [3] Hac, A. and Bodie, M., 2002. "Improvements in Vehicle Handling Through Integrated Control of Chassis Systems". *Int. J. of Vehicle Autonomous Systems*, 1(1): pp. 83-110.
- [4] Ackermann, J., Bunte, T., and Odenthal, D., 1999. "Advantages of Active Steering for Vehicle Dynamics Control". In *Proc. 32nd International Symposium on Automotive Technology and Automation*, pp. 263-270, Vienna, Austria.
- [5] Sampson, D. J. M., 2000. "Active Roll Control of Articulated Heavy Vehicles", Ph.D. Dissertation in Engineering, Cambridge University, UK.
- [6] Tibaldi, M. and Zattoni, E., 1996. "Robust Control of Active Suspensions for High Performance Vehicles," In *Proc. of the IEEE International Symposium Industrial Electronics (ISIE)*, Vol. 1., pp. 242-247.
- [7] Esmailzadeh, E. and Goodarzi, A., 2007. "Design of a VDC System for All-Wheel Independent Drive Vehicles". *IEEE/ASME Transactions on Mechatronics*, 12(6), December, pp. 632-639.
- [8] Goodarzi, A., Esmailzadeh, E., and Vossoughi, G.R., 2003. "Optimal Yaw Moment Control Law for Improved Vehicle Handling". *Mechatronics*, 13(7), September, pp. 659-675.
- [9] Esmailzadeh, E., Goodarzi, A., and Vossoughi, G.R., 2002. "Directional Stability and Control of Four-Wheel Independent Drive Electric Vehicles". *Proc Instn Mech Engrs Part K: J Multi-body Dynamics*, 216(4): pp. 303-313.
- [10] Knox, J., 2011. "Re-inventing the In-wheel Drive System". *Automotive Industries Magazine*, 190(3): p. 60.
- [11] Kim, J., 2009. "Identification of Lateral Tyre Force Dynamics Using an Extended Kalman Filter from Experimental Road Test Data". *Control Engineering Practice*. 17(3): pp. 357-367.
- [12] Tseng, H.E., Ashrafi, B., Madau, D., Brown, T. A. and Recker, D., 1999. "The Development of Vehicle Stability Control at Ford". *IEEE/ASME Transactions on Mechatronics*. 4(3): pp. 223-234.
- [13] Fukada, Y., 1999. "Slip-Angle Estimation for Vehicle Stability Control". *Vehicle System Dynamics: International Journal of Vehicle Mechanics and Mobility*, 1999. 32(4): pp.375-388.
- [14] Ray, L. R., 1995. "Nonlinear State and Tire Force Estimation for Advanced Vehicle Control," *IEEE Transactions on Control Systems Technology*, 3(1): pp. 117-124.
- [15] Ray, L. R. 1997. "Nonlinear Tire Force Estimation and Road Friction Identification: Simulation and Experiments," *Automatica*, 33(10): pp. 1819-1833.
- [16] Sill, J. and Ayalew, B., 2012. "A Saturation Balancing Control Method for Enhancing Dynamic Vehicle Stability". *Int. J. of Vehicle Design* (in press)
- [17] Pacejka, H., 2002. *Tyre and Vehicle Dynamics*. Butterworth-Heinemann, Oxford.
- [18] Borrelli, F, Baotic, M., Pekar, J. and Stewart, G., 2010. "On the Computation of Linear Model Predictive Control Laws". *Automatica*. 46(6): p. 1035-1041.
- [19] Falcone, P., Borrelli, F., Asgari, J., Tseng, H. E., and Hrovat, D., 2007. "Predictive Active Steering Control for Autonomous Vehicle Systems," *IEEE Transactions on Control Systems Technology*, 15(3): pp. 566-580.
- [20] Falcone, P. Tufo, M., Borrelli, F., Asgari, J. and Tseng, H. E., 2008. "A Linear Time Varying Model Predictive Control Approach to the Integrated Vehicle Dynamics Control Problem in Autonomous Systems," *46th IEEE Control and Decision Conference*, New Orleans, La, pp. 2980 – 2985.
- [21] Falcone, P., Tseng, H. E., Borrelli, F., Asgari, J. and Hrovat, D., 2008. "MPC-Based Yaw and Lateral Stabilisation via Active Front Steering and Braking," *Vehicle System Dynamics: International Journal of Vehicle Mechanics and Mobility*, 46(1 sup 1): pp. 611 - 628.
- [22] HongLiang, Z., and ZhiYuan, L., 2009. "Design of Vehicle Yaw Stability Controller Based on Model Predictive Control," *IEEE Intelligent Vehicles Symposium*, June3-5, Xian, China, pp. 802-807.
- [23] Maciejowski, J. M. 2002. *Predictive Control with Constraints*, Prentice Hall, Harlow, England.
- [24] Sill, J., 2012. "Predictive Tire Force Saturation Management for Vehicle Stability Control". Clemson University, Ph.D. Dissertation in Automotive Engineering, Greenville, SC.
- [25] Rill, G., 2006. "First Order Tire Dynamics", in *III European Conference on Computational Mechanics, Solids, Structures and Coupled Problems in Engineering*. June 5-8, Lisbon, Portugal.
- [26] Genta, G., 1997. *Motor Vehicle Dynamics: Modeling and Simulation*. Series on Advances in Mathematics for Applied Sciences. Vol. 43. Singapore: World Scientific Publishing